Discovery of 5-(1H-indol-5-yl)-1,3,4-thiadiazol-2-amines as potent PIM inhibitors

Bin Wu, Hui-Ling Wang, Victor Cee, Brian Lanman, Thomas Nixey, Liping Pettus, Anthony B. Reed, Ryan P. Wurz, Nadia Guerrero, Christine Sastri, Jeff Winston, J. Russell Lipford, Matthew R. Lee, Christopher Mohr, Kristin Andrews, Andrew S. Tasker

PII: S0960-894X(14)01399-7
DOI: http://dx.doi.org/10.1016/j.bmcl.2014.12.091
Reference: BMCL 22336

To appear in: *Bioorganic & Medicinal Chemistry Letters*

Received Date: 7 November 2014
Revised Date: 23 December 2014
Accepted Date: 29 December 2014

Please cite this article as: Wu, B., Wang, H-L., Cee, V., Lanman, B., Nixey, T., Pettus, L., Reed, A.B., Wurz, R.P., Guerrero, N., Sastri, C., Winston, J., Russell Lipford, J., Lee, M.R., Mohr, C., Andrews, K., Tasker, A.S., Discovery of 5-(1H-indol-5-yl)-1,3,4-thiadiazol-2-amines as potent PIM inhibitors, *Bioorganic & Medicinal Chemistry Letters* (2015), doi: http://dx.doi.org/10.1016/j.bmcl.2014.12.091

Discovery of 5-(1H-indol-5-yl)-1,3,4-thiadiazol-2-amines as potent PIM inhibitors

Bin Wu,*[a] Hui-Ling Wang,[a] Victor Cee,[a] Brian Lanman,[a] Thomas Nixey,[a] Liping Pettus,[a] Anthony B. Reed,[a] Ryan P. Wurz,[a] Nadia Guerrero,[b] Christine Sastri,[b] Jeff Winston,[b] J. Russell Lipford,[b] Matthew R. Lee,[c] Christopher Mohr,[c] Kristin Andrews,[c] and Andrew S. Tasker.[a]

Amgen Inc. One Amgen Center Drive, Thousand Oaks, California 91320-1799, USA

a) Department of Therapeutic Discovery; b) Department of Oncology; c) Department of Molecular Structure and Characterization.

* To whom correspondence should be addressed:
Bin Wu: Tel +1-805-313-5661; Fax 805-480-3016; email:binw@amgen.com

Abstract: PIM kinases are a family of Ser/Thr kinases that are implicated in tumorigenesis. The discovery of a new class of PIM inhibitors, 5-(1H-indol-5-yl)-1,3,4-thiadiazol-2-amines, is discussed with optimized compounds showing excellent potency against all three PIM isoforms.

PIM kinases are a family of serine/threonine kinases in the CAMK group (calcium/calmodulin-dependent protein kinase) that are constitutively active and are regulated at the level of transcription and translation, as opposed to the more classical post-translational phosphorylation. [1] There are three isoforms in the family, PIM1, PIM2 and PIM3, which share high homology and exhibit some functional redundancy. PIM kinases are widely expressed and are involved in a variety of biological processes, including cell survival, proliferation, differentiation and apoptosis.[2] Over-expression of PIM kinases has been reported in hematological and solid tumors such as diffuse large B-cell lymphomas (DLBCL) and prostate cancer.[3] Other evidence has also suggested that PIM kinases play a role in tumorigenesis, making it an attractive target for cancer therapy.[4] There have been several reports of both PIM1-selective and pan-PIM inhibitors, including three clinical compounds, SGI-1776, AZD1208, (structures shown in Figure 1) and LGH447 (structure not disclosed).[5,6] Considering the compensatory

nature and overlapping functions exhibited by the three PIM isoforms, we believe that pan-PIM inhibitors are of more therapeutic value. Herein, we describe our efforts in designing such agents for cancer therapy.

Figure 1. Structures of PIM inhibitors reported in clinical trials.

A high-throughput screening revealed one hit, an indazole **1**, which showed excellent activity against all three PIM kinase isoforms in HTRF assays (PIM1: 0.017 μM, PIM2: 0.031 μM and PIM3: 0.007 μM). However, **1** was found to be a multi-kinase inhibitor in our internal kinase screening panel; 7 of the 47 kinases (PKD2, GSK3-β, ROCK2, DYRK1α, CDK2, FLT3 and HGK) were inhibited more than 90% at 1 μM. A co-crystal structure of **1** and PIM1 was obtained to facilitate the design of more selective inhibitors.[7]

Figure 2. Screening hit **1** and its indole analog **2**.

The co-crystal structure revealed three key interactions between indazole **1** and the PIM1 protein (Fig. 3). The amino group on the thiazole forms an H-bond with Asp186, and the adjacent N1 engages the catalytic Lys67, while the NH on the indazole forms an H-bond with the backbone carbonyl group of Glu121. The quinoline ring resides between the glycine-rich loop and the lower hinge region with the conformation as shown. One unique feature of the PIM kinases is the presence of Pro123 at the hinge; thus ATP uses solely the NH_2 donor in this region, as opposed to the more common donor-acceptor pair of the adenine ring.[8] We reasoned that removal of N2 of the indazole ring of **1** should improve kinase selectivity. The resulting indole compound **2** indeed was devoid of activity against other kinases, yet remained moderately potent against the PIM isoforms. Thus **2** served as a useful starting point for our SAR studies with the goal to improve the potency by at least ten fold while maintaining selectivity against other kinases.

Figure 3. The co-crystal structure of compound **1** bound in the ATP binding site of unphosphorylated PIM-1 protein (PDB code: 4WSY).

Noting the presence of a crystallographic water molecule strongly hydrogen bonded to the backbone NH of Asp186, we replaced the thiazole (**2**) with a thiadiazole (**3**); this substitution resulted in improved potency against all three isoforms. Methyl amino analog **4** maintained potency, while the corresponding thiomethyl analog **5** lost significant activity presumably due to the absence of an H-bond donor for capturing the interaction with Asp186. It is noteworthy that the potency against the PIM3 isoform correlated well with IC_{50} values against PIM1, while the PIM2 isoform was more difficult to inhibit.

Table 1
PIM1, PIM2 and PIM3 inhibitory activity of substituted 3-(1H-indol-3-yl)quinolines[a]

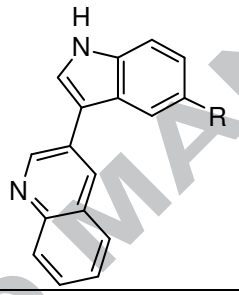

Cmpd	R	PIM1 IC_{50}(μM)	PIM2 IC_{50}(μM)	PIM3 IC_{50} (μM)
2	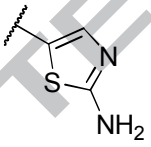	0.312	2.71	0.267
3	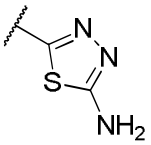	0.163	1.01	0.178
4	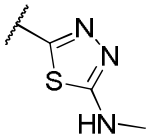	0.272	1.63	0.181
5	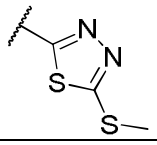	2.83	>22	4.11

[a] Data represents an average of at least two separate determinations.

In an attempt to better engage the glycine-rich loop and with the aminothiadiazole held constant, we turned our attention to the nature of the C3 substituent on the indoles. The preparation of these analogs is shown in Scheme 1. The synthesis commenced with a Suzuki coupling between boronic ester **6** and 2-bromo-5-(methylthio)-1,3,4-thiadiazole. Subsequent iodination and protection with *p*-toluenesulfonyl chloride (TsCl) gave intermediate **9**. The thiomethyl group was displaced with *p*-methoxybenzylamine ($PMBNH_2$) after oxidation with H_2O_2 and sodium tungstate. Various aromatic and heterocyclic groups were introduced at C3 of the indole through Stille coupling. Removal of the Ts and PMB protecting groups under basic and acidic conditions respectively, furnished the desired analogs.

Scheme 1. Reagents and conditions: (a) K_2CO_3 , $Pd(PPh_3)_4$, 1,4-dioxane, water, 50%; (b) I_2, KOH; (c) *p*-$MeC_6H_4SO_2Cl$, NaH, DMF, 78% for two steps; (d) H_2O_2, $NaWO_4$, AcOH; (e) *p*-$MeOC_6H_4CH_2NH_2$, dioxane, 47% for two steps; (f) R-$SnBu_3$, $Pd(PPh_3)_4$, CuI, DMF; (g) KOH, THF; (h) TFA.

Representative substituted aromatic groups at C3 to probe potential interactions with the glycine-rich loop are shown in Table 2. While the quinoline and substituted phenyl analogs (**3** and **13**) showed only moderate activity, 2-pyridyl groups substituted in the 6-position with bulky groups appeared to be most promising as exemplified by compounds **14** – **19**. Potent compounds with IC_{50} less than 100 nM in the PIM1 assay were further profiled in cellular assays measuring the inhibition of PIM1- and PIM2-dependent phosphorylation of BAD in U2OS cells.[9] Despite the high homology in the kinase domains, the three PIM isoforms show quite different ATP K_m values. In particular, PIM2 has a much lower K_m of 4 μM whereas values of 400 μM and 40 μM are observed for PIM1 and PIM3, respectively. This property renders the identification of cell active PIM2 inhibitors a challenge.[5a-5d, 5g, 5n, 5r]

The 6-aminopyridine analog **14** showed only submicromolar activity against PIM kinases, however, the introduction of a pyrrolidine in the 6-position of the pyridine ring (compound **15)** significantly improved the potency by at least 9 fold. Further improvement was seen with the 6-membered ring substitution, especially the morpholino analog with an IC_{50} of 152 nM in the PIM1 cell assay and measurable PIM2 cell potency

(7.57 μM). Introduction of primary alkylamines at 6-position of pyridine led to further improved potency in the PIM2 cell assay, with the exception of cyclohexylamine analog **19**, possibly due to the increased steric demand imposed by this substituent.

Table 2
Enzymatic and cellular activity of substituted 5-(1H-indol-5-yl)-1,3,4-thiadiazol-2-amines

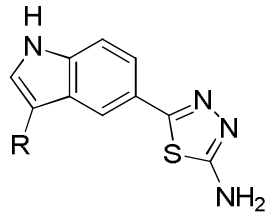

Compd	R	PIM1 IC_{50}(uM)[a]	PIM2 IC_{50}(uM)[a]	PIM3 IC_{50}(uM)[a]	PIM1cell IC_{50}(uM)	PIM2cell IC_{50}(uM)
3	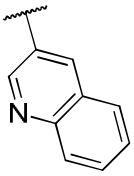	**0.163**	**1.01**	**0.178**	**2.74**	**>31.6**
13	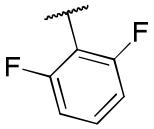	**0.177**	**0.348**	**0.097**	**ND**	**ND**
14	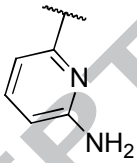	**0.865**	**0.977**	**0.186**	**ND**	**ND**
15	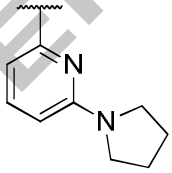	**0.048**	**0.104**	**0.015**	**0.526**	**>31.6**
16	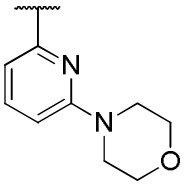	**0.016**	**0.059**	**0.006**	**0.152**	**7.57**

17	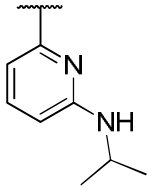	**0.024**	**0.037**	**0.005**	**0.384**	**2.19**
18	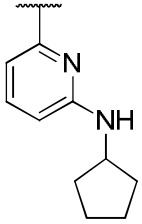	**0.012**	**0.021**	**0.005**	**0.111**	**3.09**
19	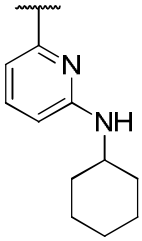	**0.109**	**0.227**	**0.022**	**ND**	**ND**
20	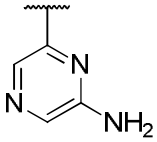	**0.142**	**0.192**	**0.029**	**ND**	**ND**
21	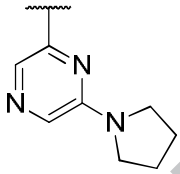	**0.011**	**0.042**	**0.009**	**0.159**	**12.1**
22	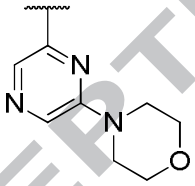	**0.005**	**0.012**	**0.004**	**0.163**	**1.90**
23	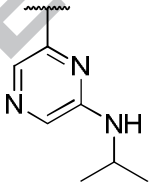	**0.002**	**0.010**	**0.001**	**0.04**	**0.945**
24	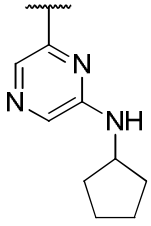	**0.001**	**0.006**	**0.001**	**0.057**	**1.22**

25	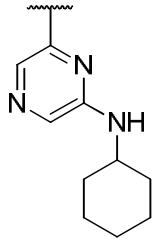	**0.004**	**0.018**	**0.002**	**0.056**	**2.60**

[a] Data represents an average of at least two separate determinations. *ND = not determined

The X-ray co-crystal structure of cyclopentyl amine analog **18** bound to PIM1 was obtained.[10] As illustrated in Figure 4, the overall binding mode is similar to screening hit **1**. N3 and N4 of the thiadiazole form a hydrogen bond network with a water molecule, Lys67 and Glu89. The 2-pyridyl system adopts a planar conformation with respect to the indole, and the aliphatic side-chain forms van der Waals contacts with the glycine-rich loop and phenyl ring of Phe49.

Figure 4. The co-crystal structure of compound **18** bound in the ATP binding site of unphosphorylated PIM1 protein (PDB code: 4WT6).

Following these results, a series of 2-amino-substituted pyrazines was prepared. As shown in Table 2, the pyrazine analogs demonstrated better potency against PIM1 and PIM2 in both biochemical and cell assays than the corresponding pyridine analogs, indicating possible more favorable water-mediated interactions between the pyrazine and extended hinge residues. Among these, both **23** and **24** exhibited single-digit nanomolar pan-PIM enzyme activity, an improvement of more than 100-fold over the original compound **2**.

We next examined O-substituted pyridine and pyrazine analogs. As shown in Table 3, the optimal affinities for the three PIM kinases were achieved with isopropoxy substitution. Smaller substituents, such as methoxy and ethoxy groups, or larger substituents such as cyclobutoxy and cyclopentoxy led to various degrees of erosion of PIM inhibitor potency. In addition, substitution at the C5 pyrazine position (**33**) resulted in significant loss of activity, presumably due to lack of contact with the glycine-rich loop.

Table 3
PIM inhibitory activity of O-substituted 5-(3-(pyridin-2-yl)-1H-indol-5-yl)-1,3,4-thiadiazol-2-amines and 5-(3-(pyrazin-2-yl)-1H-indol-5-yl)-1,3,4-thiadiazol-2-amines

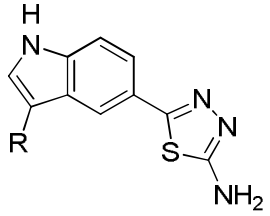

Compd	R	PIM1 IC_{50} (uM)[a]	PIM2 IC_{50} (uM)[a]	PIM3 IC_{50} (uM)[a]	PIM1 cell IC_{50} (uM)	PIM2 cell IC_{50} (uM)
26	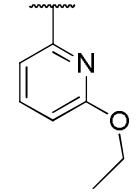	**0.017**	**0.022**	**0.003**	**0.141**	**3.73**
27	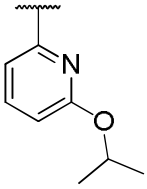	**0.007**	**0.010**	**0.002**	**0.106**	**2.22**
28	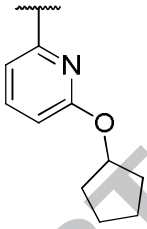	**0.015**	**0.041**	**0.005**	**0.479**	**6.90**
29	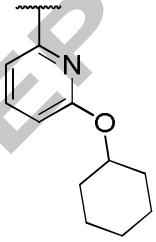	**0.041**	**0.114**	**0.018**	**1.02**	**>31.6**
30	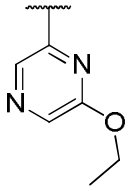	**0.021**	**0.028**	**0.008**	**0.20**	**2.75**

31	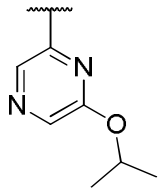	**0.008**	**0.017**	**0.003**	**0.092**	**2.22**
32	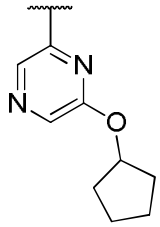	**0.011**	**0.025**	**0.011**	**0.176**	**6.54**
33	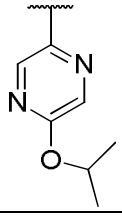	**0.262**	**1.29**	**0.185**	**ND**	**ND**

[a] Data represents an average of at least two separate determinations.

In a subsequent kinase profiling experiment using custom KINOMEscan[sm] assay, the two lead compounds **23** and **27** exhibited good kinase selectivity with selectivity score of 0.07 and 0.05, respectively (S(35) at1 μM, 100 kinases).[11]

In summary, we have discovered 5-(1H-indol-5-yl)-1,3,4-thiadiazol-2-amines as a novel class of pan-PIM inhibitors. Starting from the screening hit **1**, with the aid of crystallographic information we quickly designed indole **2** with favorable kinase selectivity profile. Focused SAR study identified compounds **23** and **27** with over 100 fold improvement in inhibitory activity against all three PIM isoforms. Further studies of these inhibitors will be reported in due course.

Acknowledgments The authors thank Randy Hungate, Philip Tagari and Christian Romel for their support for this research program. Thanks also go to Randy Jensen and Chris Wilde for spectroscopic assistance.

Supplementary data X-Ray data for the co-crystal structure of compound **1** and **18** in Pim-1 protein and PIM enzyme assays experimental details.

References and notes

1. (a) Cuypers, H. T.; Selten, G.; Quint, W.; Zijlstra, M.; Maandag, E. R.; Boelens, W.; van Wezenbeek, P.; Melief, C.; Berns, A. *Cell* **1984**, *37*, 141; (b) Zhukova, Y. N.; Alekseeva, M. G.; Zakharevich, N. V.; Shtil, A. A.; Danilenko, V. N. *Mol. Bio.* **2011**, *45*, 695.
2. Fox, C. J.; Hammerman, P. S.; Cinalli, R. M.; Master, S. R.; Chodosh, L. A.; Thompson, C. B. *Genes & Dev.* **2003**, *17*, 1841.
3. Brault, L.; Gasser, C.; Bracher, F.; Huber, K.; Knapp, S.; Schwaller, J. *Haematologica* **2010**, *95*, 1004.
4. Nawijn, M. C.; Alendar, A.; Berns, A. *Nat. Rev. Cancer* **2011**, *11*, 23.

5 (a) Drygin, D.; Haddach, M.; Pierre, F.; Ryckman, D. M. *J. Med. Chem.* **2012**, *55*, 8199; (b) Xia, Z.; Knaak, C.; Ma, J.; Beharry, Z. M.; McInnes, C.; Wang, W.; Kraft, A. S.; Smith, C. D. *J. Med. Chem.* **2009**, *52*, 74; (c) Qian, K.; Wang, L.; Cywin, C. L.; Farmer, B. T., II; Hickey, E.; Homon, C.; Jakes, S.; Kashem, M. A.; Lee, G.; Leonard, S.; Li, J.; Magboo, R.; Mao, W.; Pack, E.; Peng, C.; Prokopowicz, A., III; Welzel, M.; Wolak, J.; Morwick, T. *J. Med. Chem.* **2009**, *52*, 1814; (d) Tao, Z.-F.; Hasvold, L. A.; Leverson, J. D.; Han, E. K.; Guan, R.; Johnson, E. F.; Stoll, V. S.; Stewart, K. D.; Stamper, G.; Soni, N.; Bouska, J. J.; Luo, Y.; Sowin, T. J.; Lin, N.-H.; Giranda, V. S.; Rosenberg, S. H.; Penning, T. D. *J. Med. Chem.* **2009**, *52*, 6621; (e) Nishiguchi, G. A.; Atallah, G.; Bellamacina, C.; Burger, M. T.; Ding, Y.; Feucht, P. H.; Garcia, P. D.; Han, W.; Klivansky, L.; Lindvall, M. *Bioorg. Med. Chem. Lett.* **2011**, *21*, 6366; (e) Pierre, F.; Stefan, E.; Nédellec, A. S.; Chevrel, M. C.; Regan, C. F.; Siddiqui-Jain, A.; Macalino, D.; Streiner, N.; Drygin, D.; Haddach, M.; O'Brien, S. E.; Anderes, K.; Ryckman, D. M. *Bioorg. Med. Chem. Lett.* **2011**, *21*, 6687; (f) Pastor, J.; Oyarzabal, J.; Saluste, G.; Alvarez, R. M.; Rivero, V.; Ramos, F.; Cendón, E.; Blanco-Aparicio, C.; Ajenjo, N.; Cebriá, A.; Albarrán, M. I.; Cebrián, D.; Corrionero, A.; Fominaya, J.; Montoya, G.; Mazzorana, M. *Bioorg. Med. Chem. Lett.* **2012**, *22*, 1591; (g) Tsuhako, A. L.; Brown, D. S.; Koltun, E. S.; Aay, N.; Arcalas, A.; Chan, V.; Du, H.; Engst, S.; Franzini, M.; Galan, A.; Huang, P.; Johnston, S.; Kane, B.; Kim, M. H.; Laird, A. D.; Lin, R.; Mock, L.; Ngan, I.; Pack, M.; Stott, G.; Stout, T. J.; Yu,

P.; Zaharia, C.; Zhang, W.; Zhou, P.; Nuss, J. M.; Kearney, P. C.; Xu, W. *Bioorg. Med. Chem. Lett.* **2012**, *22*, 3732; (h) Dakin, L. A.; Block, M. H.; Chen, H.; Code, E.; Dowling, J. E.; Feng, X.; Ferguson, A. D.; Green, I.; Hird, A. W.; Howard, T.; Keeton, E. K.; Lamb, M. L.; Lyne, P. D.; Pollard, H.; Read, J.; Wu, A. J.; Zhang, T.; Zheng, X. *Bioorg. Med. Chem. Lett.* **2012**, *22*, 4599; (i) Nakano, H.; Saito, N.; Parker, L.; Tada, Y.; Abe, M.; Tsuganezawa, K.; Yokoyama, S.; Tanaka, A.; Kojima, H.; Okabe, T.; Nagano, T. *J. Med. Chem.* **2012**, 55, 5151; (j) Letribot, B.; Akué-Gédu, R.; Santio, N. M.; El-Ghozzi, M.; Avignant, D.; Cisnetti, F.; Koskinen, P. J.; Gautier, A.; Anizon, F.; Moreau, P. *Eur. J. Med. Chem*. **2012**, *50*, 304; (k) Li, R.; Martin, M. P.; Liu, Y.; Wang, B.; Patel, R. A.; Zhu, J.-Y.; Sun, N.; Pireddu, R.; Lawrence, N. J.; Li, J.; Haura, E. B.; Sung, S.-S.; Guida, W. C.; Schonbrunn, E.; Sebti, S. M. *J. Med. Chem.* **2012**, *55*, 2474; (l) Haddach, M.; Michaux, J.; Schwaebe, M. K.; Pierre, F.; O'Brien, S. E.; Borsan, C.; Tran, J.; Raffaele, N.; Ravula, S.; Drygin, D.; Siddiqui-Jain, A.; Darjania, L.; Stansfield, R.; Proffitt, C.; Macalino, D.; Streiner, N.; Bliesath, J.; Omori, M.; Whitten, J. P.; Anderes, K.; Rice, W. G.; Ryckman, D. M. *ACS Med. Chem. Lett.* **2012**, *3*, 135; (m) Suchaud, V.; Gavara, L.; Saugues, E.; Nauton, L.; Théry, V.; Anizon F.; Moreau, P. *Bioorg. Med. Chem.* **2013**, *21*, 4102; (n) Casuscelli F.; Ardini, E.; Avanzi, N.; Casale, E.; Cervi, E.; D'Anello, M.; Donati, D.; Faiardi, D.; Ferguson, R. D.; Fogliatto, G.; Galvani,A.; Marsiglio, A.; Mirizzi, D. G.; Montemartini, M.; Orrenius, C.; Papeo, G.; Piutti, C.; Salom, B.; Felder, E. R. *Bioorg. Med. Chem.* **2013**, *21*, 7364; (o) Gavara, L.; Suchaud, V.; Nauton, L.; Nauton, L.; Théry, V.; Anizon F.; Moreau, P. *Bioorg. Med. Chem.* **2013**, *23*, 2298; (p) Wang, X.; Magnuson, S.; Pastor, R.; Fan, E.; Hu, H.; Tsui, V.; Deng, W.; Murray, J.; Steffek,M.; Wallweber, H.; Moffat, J.; Drummond, J.; Chan, G.; Harstad, E.; Ebens, A. J. *Bioorg. Med. Chem. Lett.* **2013**, *23*, 3149; (q) Dwyer, M. P.; Keertikar, K.; Paruch, K.; Alvarez, C.; Labroli, M.; Poker, C.; Fischmann, T. O.; Mayer-Ezell, R.; Bond, R.; Wang, Y.; Azevedo, R. Guzi, T. J. *Bioorg. Med. Chem. Lett.* **2013**, *23*, 6178. (r) Burger, M. T.; Han, W.; Lan, J.; Nishiguchi, G.; Bellamacina, C.; Lindval, M.; Atallah, G.; Ding, Y.; Mathur, M.; McBride, C.; Beans, E. L.; Muller, K.; Tamez, V.; Zhang, Y.; Huh, K.; Feucht, P.;

Zavorotinskaya, T.; Dai, Y.; Holash, J.; Castillo, J.; Langowski, J.; Wang, Y.; Chen, M. Y.; Garcia, P. D. *ACS Med. Chem. Lett.* **2013**, *4*, 1193.

6 (a) Chen, L. S.; Redkar, S.; Bearss, D.; Wierda, W. G.; Gandhi, V. *Blood* **2009**, *114*, 4150; (b) Keeton, E. K.; McEachern, K.; Dillman, K. S.; Palakurthi, S.; Cao, Y.; Grondine, M. R.; Kaur, S.; Wang, S.; Chen, Y.; Wu, A.; Shen, M.; Gibbons, F. D.; Lamb, M. L.; Zheng, X.; Stone, R. M.; DeAngelo, D. J.; Platanias, L. C.; Dakin, L. A.; Chen. H.; Lyne, P. D. Huszar, D. *Blood* **2014**, *123*, 905.

7 Atomic coordinates and structure factors for crystal structures of compound 1 bound to PIM1 can be accessed using PDB code 4WSY. Figure 3 was generated with The PyMOL Molecular Graphics System, Version 1.7.0.1 Schrödinger, LLC.

8 Qian, K. C.; Wang, L.; Hickey, E. R.; Studts, J.; Barringer, K.; Peng, C.; Kronkaitis, A.; Li, J.; White, A.; Mische, S.; Farmer, B. *J. Biol. Chem.* **2005**, *280*, 6130.

9 (a) The cell lines used in the assay were generated by the stable transfection of either Pim-1 or Pim-2 into the U2OS human osteogenic sarcoma line. (b) Aho, T. L. T.; Sandholm, J.; Peltola, K. J.; Mankonen, H. P.; Lilly, M.; Koskinen, P. J. *FEBS Lett.* **2004**, *571*, 43; (c) Yan, B.; Zemskova, M.; Holder, S.; Chin, V.; Kraft, A.; Koskinen, P. J.; Lilly, M. *J. Biol. Chem.* **2003**, *278*, 45358.

10 Atomic coordinates and structure factors for crystal structures of compound **18** bound to PIM1 can be accessed using PDB code 4WT6. Figure 4 was generated with The PyMOL Molecular Graphics System, Version 1.7.0.1 Schrödinger, LLC.

11 Assays were performed utilizing KINOMEscan^{sm}. Activity is recorded via a competition binding assay of selected kinases that are fused to a proprietary tag. POC values are determined by measurements of the amount of kinase bound to an immobilized, active-site directed ligand in the presence and absence of the test compound. Selectivity score was calculated by dividing the number of kinases that compounds bind to by the total number of distinct kinases tested, excluding mutant variants. S(35) = (number of non-mutant kinases with %Ctrl <35)/(number of non-mutant kinases tested).

Figure 1. Structures of PIM inhibitors reported in clinical trials.

Figure 2. Screening hit **1** and its indole analog **2**.

Figure 3. The co-crystal structure of compound **1** bound in the ATP binding site of unphosphorylated PIM-1 protein (PDB code: 4WSY).

Figure 4. The co-crystal structure of compound **18** bound in the ATP binding site of unphosphorylated PIM1 protein (PDB code: 4WT6).

Scheme 1. Reagents and conditions: (a) K_2CO_3 , $Pd(PPh_3)_4$, 1,4-dioxane, water, 50%; (b) I_2, KOH; (c) *p*-$MeC_6H_4SO_2Cl$, NaH, DMF, 78% for two steps; (d) H_2O_2, $NaWO_4$, AcOH; (e) *p*-$MeOC_6H_4CH_2NH_2$, dioxane, 47% for two steps; (f) R-$SnBu_3$, $Pd(PPh_3)_4$, CuI, DMF; (g) KOH, THF; (h) TFA.

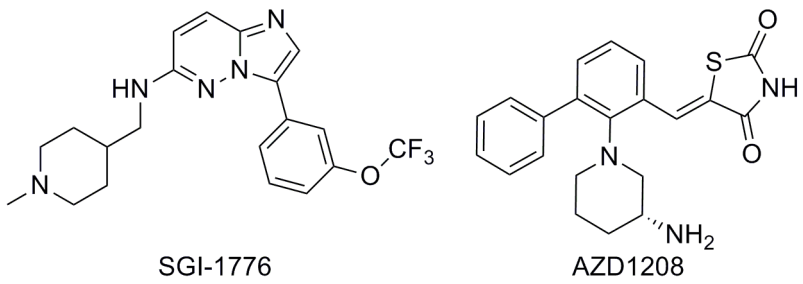

Figure 1. Structures of PIM inhibitors reported in clinical trials.

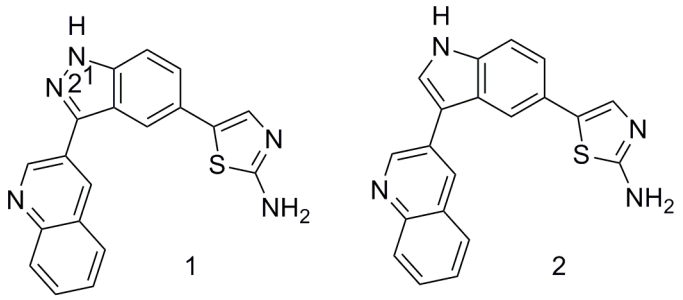

PIM1 IC50 = 0.017 mM	PIM1 IC50 = 0.312 mM
PIM2 IC50 = 0.031 mM	PIM2 IC50 = 2.71 mM
PIM3 IC50 = 0.007 mM	PIM3 IC50 =0.267 mM

Figure 2. Screening hit **1** and its indole analog **2**.

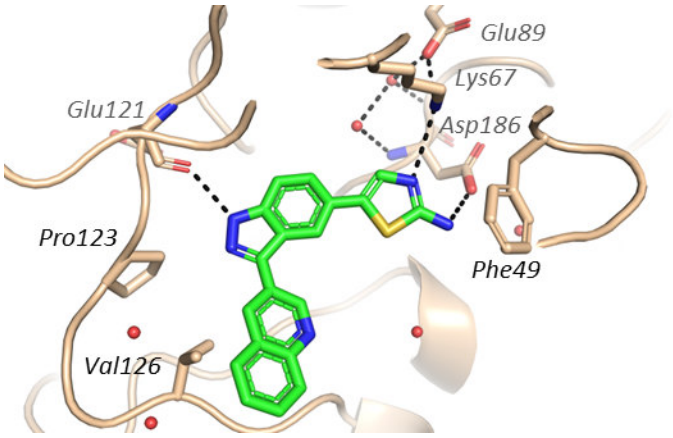

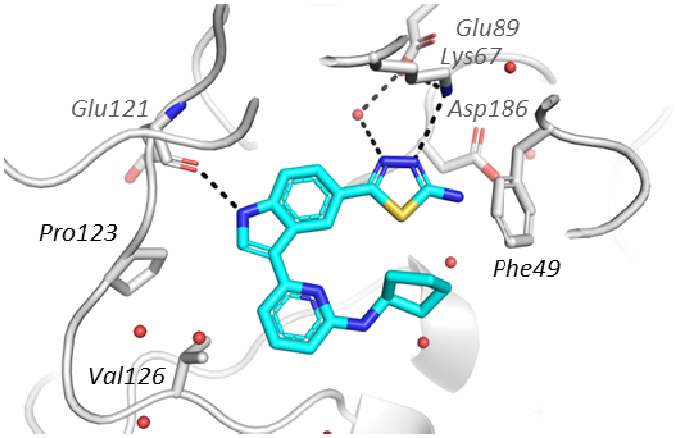

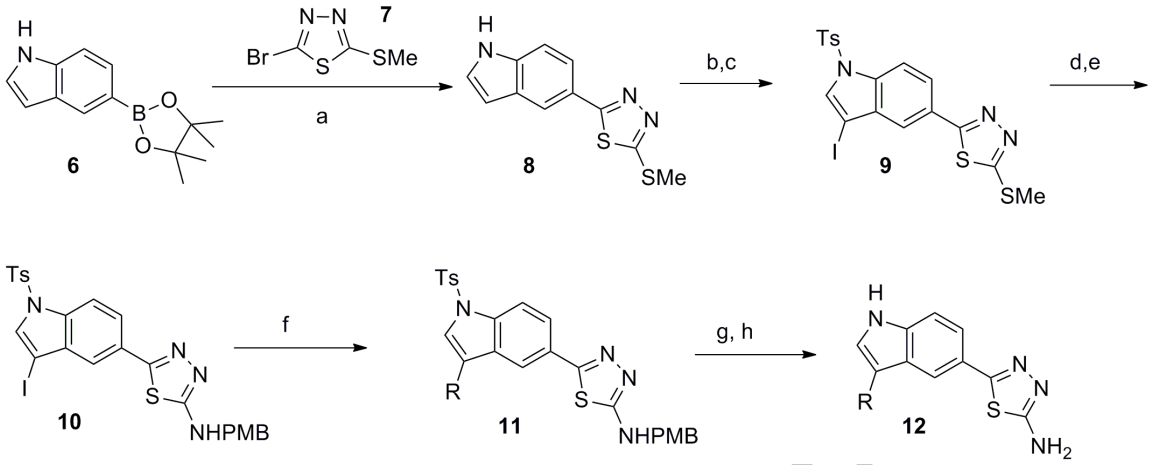

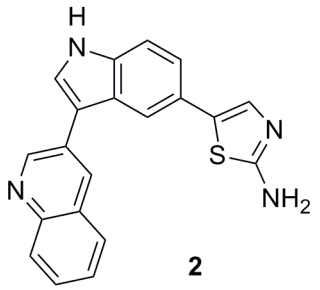

2

PIM1 IC_{50} = 0.312 μM
PIM2 IC_{50} = 2.71 μM
PIM3 IC_{50} = 0.267 μM

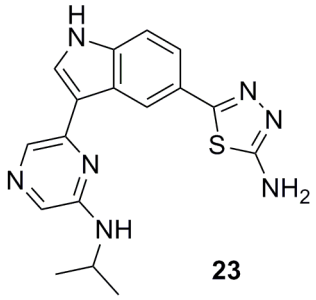

23

PIM1 IC_{50} = 0.002 μM
PIM2 IC_{50} = 0.01 μM
PIM3 IC_{50} = 0.001 μM